Graefe's Archive for Clinical and Experimental Ophthalmology
https://doi.org/10.1007/s00417-018-4134-2

BASIC SCIENCE

A new immunodeficient retinal dystrophic rat model for transplantation studies using human-derived cells

Biju B. Thomas[1,2] · Danhong Zhu[1,3] · Tai-Chi Lin[1,2,4,5] · Young Chang Kim[1,3] · Magdalene J. Seiler[6,7] · Juan Carlos Martinez-Camarillo[1,2] · Bin Lin[6,7] · Yousuf Shad[8] · David R. Hinton[1,3] · Mark S. Humayun[1,2]

Received: 8 December 2017 / Revised: 28 August 2018 / Accepted: 3 September 2018

Abstract

Purpose To create new immunodeficient Royal College of Surgeons (RCS) rats by introducing the defective MerTK gene into athymic nude rats.

Methods Female homozygous RCS (RCS-p+/RCS-p+) and male nude rats (Hsd:RH-*Foxn1*^{mu}, mutation in the foxn1 gene; no T cells) were crossed to produce heterozygous F1 progeny. Double homozygous F2 progeny obtained by crossing the F1 heterozygotes was identified phenotypically (hair loss) and genotypically (RCS-p+ gene determined by PCR). Retinal degenerative status was confirmed by optical coherence tomography (OCT) imaging, electroretinography (ERG), optokinetic (OKN) testing, superior colliculus (SC) electrophysiology, and by histology. The effect of xenografts was assessed by transplantation of human embryonic stem cell-derived retinal pigment epithelium (hESC-RPE) and human-induced pluripotent stem cell-derived RPE (iPS-RPE) into the eye. Morphological analysis was conducted based on hematoxylin and eosin (H&E) and immunostaining. Age-matched pigmented athymic nude rats were used as control.

Results Approximately 6% of the F2 pups (11/172) were homozygous for RCS-p+ gene and Foxn1^{mu} gene. Homozygous males crossed with heterozygous females resulted in 50% homozygous progeny for experimentation. OCT imaging demonstrated significant loss of retinal thickness in homozygous rats. H&E staining showed photoreceptor thickness reduced to 1–3 layers at 12 weeks of age. Progressive loss of visual function was evidenced by OKN testing, ERG, and SC electrophysiology. Transplantation experiments demonstrated survival of human-derived cells and absence of apparent immune rejection.

Conclusions This new rat animal model developed by crossing RCS rats and athymic nude rats is suitable for conducting retinal transplantation experiments involving xenografts.

Keywords Human-derived cells · Immunodeficiency · Retinal dystrophy · Retinal transplantation

Introduction

Age-related macular degeneration (AMD) and retinitis pigmentosa (RP) lead to a profound loss of vision in millions worldwide. Many of these patients require replacement of both retinal pigment epithelium (RPE) and photoreceptors (PRs). Cell-based techniques for the replacement of RPE, photoreceptors, and other inner retinal cells have been a major focus for various research groups [1–4]. Promising techniques are now emerging with the potential to replace even retinal

✉ Biju B. Thomas
biju.thomas@med.usc.edu

1 Department of Ophthalmology, USC Roski Eye Institute, University of Southern California, Los Angeles, CA 90033, USA

2 USC Institute for Biomedical Therapeutics, University of Southern California, Los Angeles, CA, USA

3 Department of Pathology, Keck School of Medicine, University of Southern California, Los Angeles, CA, USA

4 Department of Ophthalmology, Taipei Veterans General Hospital, Taipei, Taiwan, Republic of China

5 Institute of Clinical Medicine, National Yang-Ming University, Taipei, Taiwan, Republic of China

6 Department of Physical Medicine & Rehabilitation, University of California-Irvine, Irvine, CA, USA

7 Stem Cell Research Center, University of California-Irvine, Irvine, CA, USA

8 Department of Chemistry and Chemical Biology, McMaster University, Hamilton, ON, Canada

Published online: 13 September 2018

ganglion cells and their axons in the optic nerve [5]. Other approaches are aimed at curing retinal degenerative (RD) diseases based on the transplantation of retinal progenitor cells (RPCs). Transplantation studies involving both RPE and retinal progenitor cells have been demonstrated in animal models [4, 6–8] and humans [9] by grafting sheets of fetal-derived neural retinal progenitor cells with its RPE.

The dystrophic Royal College of Surgeons (RCS) rats [10, 11] and various lines of transgenic S334ter rats [12–14] are the most commonly used rat disease models in ophthalmic research. These models are commonly used for the assessment of beneficial effects of cell replacement therapies [15–22]. The dystrophic RCS rats are characterized by RPE dysfunction due to the deletion in the Mer tyrosine kinase (MerTK) receptor that abolishes internalization of PR outer segments by RPE cells [23]. The phagocytosis of shed photoreceptor outer segments (OS) is a prerequisite for maintaining normal retinal physiology for which RPE plays a major role. Accumulation of debris in the subretinal space can lead to severe photoreceptor degeneration and rapid loss of vision. In RCS rats, although retinal thickness remains close to the level of normal eyes at 1 month of age [24, 25], the outer nuclear layer (ONL) is reduced to a single layer at the age of 3 months, with the debris zone occupying the former outer segment area. Finally, at 6 months, the inner nuclear layer is in direct contact with the RPE cell layer, with very few photoreceptors surviving [26–30].

Although the retina is considered an immune privileged area, some immunological reactions to xenograft can occur. Most of the preclinical studies involving human-derived cells used animal models that are exposed to severe immunosuppression regimes [31, 32]. Based on the studies conducted in our laboratory, administration of immunosuppressants in rodents can yield only partial success because of the inconsistent blood immunosuppression levels. The procedure itself is labor intensive and may cause additional pain and discomfort to the animals. Based on a recent investigation, a standard regimen of cyclosporine A plus dexamethasone administered to RCS rats resulted in demonstrable systemic side effects and depressed scores on behavioral and electrophysiological testing [33]. Further, according to Anderson et al. [34], the presence of an active immunorejection response itself may significantly alter the efficacy and critically, the safety profile of the cell therapy candidate. Recently, Zhu et al. [35] demonstrated that using an immunodeficient model enhances long-term functional integration of human embryonic stem cell (hESC)-derived PRs. The above findings suggest the importance of using immunodeficient models for testing replacement therapies involving human-derived cells. The only immunodeficient RD rat model currently available is S334ter line-3 rats [36], a model for photoreceptor degeneration showing certain similarities to human retinitis pigments (RP). Contrary to this, the RCS rats are considered as a model suitable for studying RPE dysfunction/disease and early stage interventions based on RPE replacement. Here, we report creating an immunodeficient rat model that manifests the dystrophic features of RCS rats and hence can be considered as desirable for conducting xenograft studies.

Methods

Animals

Breeding pairs of pigmented dystrophic RCS rats (RCS-p+) were obtained from Dr. Mat LaVail (University of California, San Francisco, USA). Pigmented athymic nude rats (Hsd:RH-Foxn1^{mu}, mutation in the foxn1 gene; no T cells) were purchased from Harlan Laboratories, NJ, USA. All experiments were approved by the University of Southern California Institutional Animal Care and Use Committee (IACUC) and were performed in accordance with the National Institutes of Health Guide for the Care and Use of Laboratory Animals and the ARVO Statement for the Use of Animals in Ophthalmic and Vision Research.

Breeding scheme

Adult female RCS rats were mated with athymic nude male rats. Males and females of the F1 progeny from different litters were crossed to produce F2 generation. RCS-p+ gene status of the pups was identified by genotyping. Immunodeficiency status was established based on phenotypic expression (hair loss). Since immunodeficient females are incapable of raising pups, only heterozygous females (phenotypically non-immunodeficient) were used in all subsequent breeding. These females were crossed with double homozygous (immunodeficient and retinal dystrophic) males to produce approximately 50% double homozygous (dystrophic and immunodeficient) pups. All rats were kept in an aseptic and temperature-controlled environment.

Genotyping

The genotyping for RCS/MerTK-alleles was performed with the RRRC (Rat Resource & Research Center) 662 protocol and with the PCR-RFLP assay reported by Hirasawa et al. previously [37], see Table 1 for details.

Retinal thickness measured using optical coherence tomography imaging

Spectral domain optical coherence tomography (SD-OCT) images of the retina were obtained using a Bioptigen Envisu R2200 spectral domain ophthalmic imaging system (Bioptigen, Research Triangle Park, NC). Rats were

Table 1 The primers used for genotyping RCS and nude genes

Genes	Allele	Primers
Mertk (RCS)	Mutant	Forward: 5′-TGG GAC TAG CCT CAG TTC AC-3′
		Reverse: 5′-CAC TCT CTG GTA GCC ATT G-3′
	Wild type	Forward: 5′-ATC ACA TCC AGC ACA CAC AG-3′
		Reverse: 5′-CAC TCT CTG GTA GCC ATT G-3′
Foxn1 (nude)	Mutant and wild type	Forward: 5′-CACCAGCAGCCATTGTTGTCA-3′
		Reverse: 5′-CATGGTCCTGGCTGAGGAAG-3′

anesthetized, and pupils were dilated using 1% atropine drops (Akorn Pharmaceuticals, Lake Forest, IL). During imaging, the animals were placed on a movable platform that allowed easy maneuvering of the head. The eyes were protected by a frequent application of Systane ® (Alcon) to minimize the refractive errors and avoid ocular damage by keeping the cornea moist. From each eye, five scan acquisitions were taken. Areas of 2.6 mm × 2.6 mm were imaged with one of the three following scan parameters (units are # B-scans/# A-scans/B-scan averaging value): 488 × 488 × 5 (optimal for obtaining maximum projection fundus image); 700 × 70 × 25; and 800 × 20 × 80 (optimal for obtaining retinal cross sections).

Optokinetic testing

Optokinetic (OKN) testing was performed at three different time points as previously described [38]. An EthoVision® XT, Noldus Information Technology computer program was used to generate alternate black and white stripes. The head-tracking responses during clockwise (1 min) and anti-clockwise (1 min) stripe rotations were recorded using a digital camcorder. Visual acuity was tested by the decrease of stripe width at 0.5 decrements. Video recordings were evaluated to compute the head-tracking scores by two separate investigators whom were both blind to the experimental condition.

Electroretinography testing

Electroretinography (ERG) was performed every month after birth using the HMsERG system (Ocuscience, Las Vegas, NV) as previously described [8]. Briefly, after dark adapted overnight, the rats were anesthetized with an injection of ketamine/xylazine (37.5 mg/kg ketamine and 5 mg/kg xylazine, i.p.) and 0–2% isoflurane mixed with oxygen through a gas anesthesia mask (Stoelting, Wood Dale, IL, USA); and eyes were dilated using tropicamide 1% (Bausch & Lomb Inc., Tampa, FL) eye drops. Contact lens electrodes were placed on the cornea of both eyes, with reference and ground electrodes placed subcutaneously. An optically clear ophthalmic gel was used to maintain hydration and conductivity between the cornea and recording electrodes. Scotopic testing was conducted with flash stimuli intensities ranging from 1 to 25,000 millicandela (mcd) followed by photopic testing (light adaptation of 10 min prior to the photopic test which records flash stimuli responses of 10–25,000 mcd).

Superior colliculus electrophysiology

Electrophysiological mapping of the superior colliculus (SC) was performed at about 21 weeks post-surgery. During SC mapping, the responses were recorded from approximately 30 different SC locations. At each location, the recordings were made at varying light intensity (~ 0.25 steps) to obtain a luminance threshold map of the SC as described previously [7, 39, 40].

Preparation of iPS-RPE and hESC-RPE cell suspension

The iPS cell line generated from healthy adult fibroblast cells and differentiated into RPE cells (frozen passage 2 cells) was obtained from Dr. Kapil Bharti (National Institute of Health, Bethesda, MD, USA) [41, 42]. Human embryonic stem cells (NIH-registered H9 cell line, WiCell Research Institute, Inc., Madison, WI, USA) were allowed to spontaneously differentiate into RPE cells. Passage 3 iPSC-RPE and hESC-RPE that had been cultured in vitronectin-coated culture dishes for 4 weeks were used for subretinal injections. The cells were dissociated from the culture dishes by TrypLE (Life Technologies) and suspended in DMEM/F12 medium to a final concentration of 5×10^7 cells/mL.

Cell suspension injection in RCS rats

Male and female double homozygous (immunodeficient) RCS rats (P28–P30) were used for iPS-RPE ($n = 8$) and hESC-RPE ($n = 5$) cell suspension injection experiments. Immunodeficient RCS rats (no surgery, $n = 5$) and non-immunodeficient RCS rats (hESC-RPE suspension injection, $n = 5$) were used as control groups. The rats were anesthetized and placed under a surgical microscope, and their pupils were pharmacologically dilated. A temporal peritomy was made on the left eye, and the superior and lateral recti were isolated. A 4–0 silk suture was passed under these two muscles and used to mechanically hold the eye in the desired position. A 27-

gauge needle was used to make a scleral incision of approximately 1.2 mm, approximately 1.5 mm posterior to the limbus at the temporal equator. An anterior chamber paracentesis was performed to lower the intraocular pressure. A 32-gauge needle was then inserted into the subretinal space through the aforementioned scleral incision. Two microliters of cell mixture containing approximately 10^5 cells was injected into the subretinal space. Successful injection created a local retinal detachment (bleb) that was confirmed during fundus examination.

Histological assessments

Anesthetized animals were euthanized with intracardiac injection of 0.5 mL pentobarbital sodium 390 mg and phenytoin sodium 50 mg (Euthasol; Virbac AH, Inc., Fort Worth, TX). Both right and left eyes were enucleated and fixed using Davidson's solution for at least 18 h before embedded in paraffin. Microtome sections (5 μm thickness) passing through the center of optic nerve were stained using hematoxylin and eosin (H&E), and adjacent slides were used for immunostaining. TRA-1-85 (human-specific marker), RPE65 (RPE-specific marker), CD68 (macrophage-specific marker), and GFAP (glial cell-specific marker) primary antibodies were used for immunofluorescence assays. H&E-stained retinal sections were imaged with an Aperio ScanScope, and immunofluorescent-stained sections were imaged using a digital microscope BZ-X700 E (Keyence America, IL, USA).

Statistics

Statistical comparisons were made using Graphpad Prism software (Graphpad Software Inc., La Jolla, CA). Paired *t* test was used for analyzing the OKN data. Rest of the data was analyzed using Student's *t* test or analysis of variance (ANOVA) followed by appropriate post hoc test. For all comparisons, the significance level was determined at $p < 0.05$. Age-matched normal pigmented athymic nude rats were used as controls for all experiments.

Results

Breeding of immunodeficient RCS rats

Successful crossbreeding between dystrophic RCS rats and immunodeficient athymic nude rats (Fig. 1) was possible as evidenced by normal litter size (6–13 pups per litter), pup survival, and age of weaning. Immunodeficient pups (phenotypically discernable based on hair loss) were smaller in body size compared to their non-immunodeficient counterparts. Based on genotypic (Fig. 2) and phenotypic characteristics, the double homozygotes were identified from the F2 progeny. Based on this, 6% of the F2 pups (11/172) homozygous for RCS-p+ gene also showed phenotypic features of nude rats (hairlessness) and hence considered as double homozygous (immunodeficient RCS rats).

Dystrophic characteristics of immunodeficient RCS rats based on histological analysis

In RCS rats, retinal degeneration starts early in life and progresses quickly. In the new double homozygous RCS model (RCS-p+ gene and features of nude rats confirmed), signs of photoreceptor loss were observed at the age of P28 (Fig. 3b). Only 2–3 layers of outer nuclei were present at the age of 2 months (Fig. 3c). More or less complete loss of photoreceptors was observed after the age of 4 months (Fig. 3d).

Progressive loss of retinal thickness in immunodeficient RCS rats demonstrated by OCT imaging

OCT imaging was performed in dystrophic (RCS) immunodeficient rats at various postnatal time points. At the age of 1 month (Fig. 4b), the retinal thickness was comparable to that of age-matched non-dystrophic immunodeficient rats (non-dystrophic athymic nude rat, Fig. 4a). Considerable loss of retinal thickness was observed in these rats when assessed at the age of 2 months (Fig. 4c). Progressive loss of retinal thickness was observed in immunodeficient RCS rats tested during the subsequent time points (Fig. 4d–f). Quantitative measurement of retinal thickness made using cross-sectional OCT images also showed significant loss of retinal thickness in 3-month-old immunodeficient RCS rats compared to non-dystrophic immunodeficient (athymic nude) rats ($p < 0.001$, Fig. 5). The above observations are consistent with the pattern of retinal dystrophy observed in non-immunodeficient RCS rats [43, 44].

Visual functional loss in double homozygous rats demonstrated by optokinetic testing

The visual functional deficit in RCS nude rats was shown by severe loss of OKN visual acuity (Fig. 6). Although OKN visual activity initially (up to postnatal, P45) remained close to the level of normal rats, significant decrease in visual function was observed after P60. No apparent OKN visual behavioral activity was noticed after the age of 6 months.

Electroretinography testing in immunodeficient RCS rats showed progressive loss of retinal function

Electroretinography (ERG) recording was conducted in immunodeficient RCS rats once a month. The immunodeficient

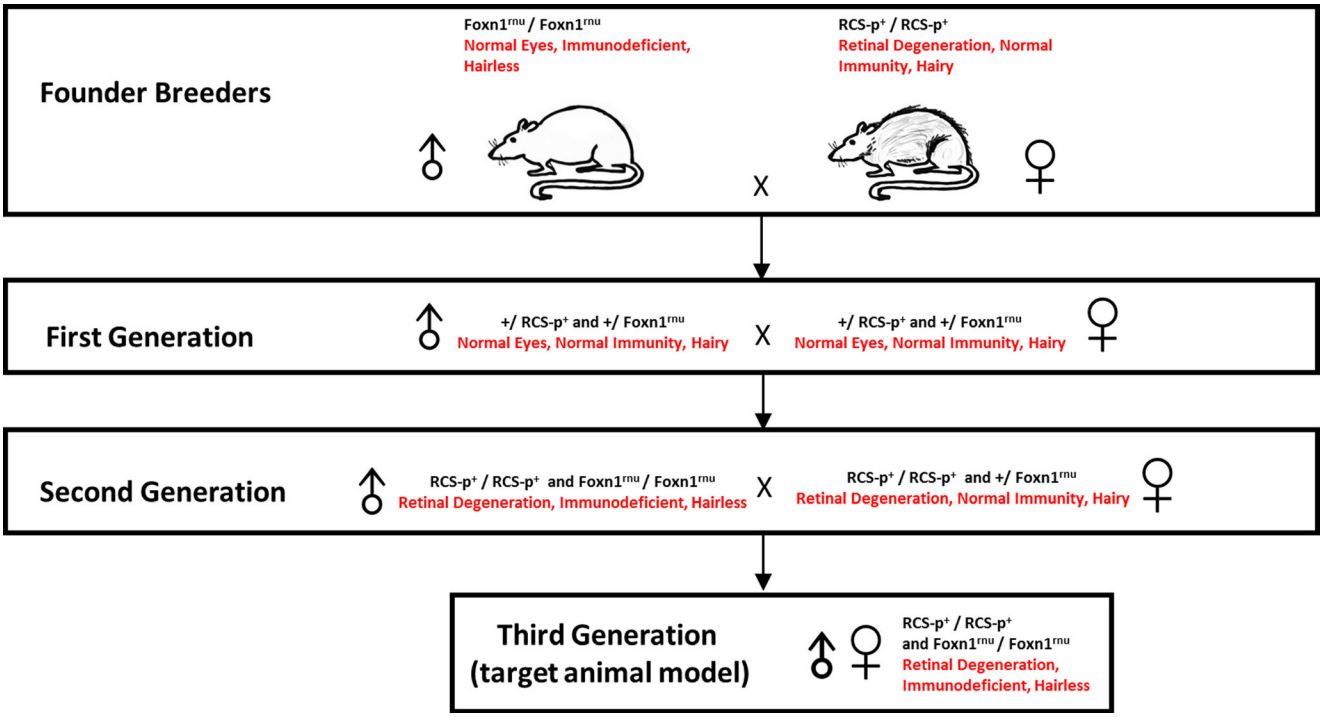

Fig. 1 Breeding scheme employed to generate immunodeficient RCS rats. Initial mating experiments were conducted using male athymic nude rats (Hsd:RH-Foxn1^{mu}) and female dystrophic RCS rats (RCS-p+ strain, Mat LaVail, UCSF) to generate F1 pups. The F1 rats were crossed to generate F2 litters. Pups that are double homozygous (homozygous for RPE dysfunction disease and immunodeficiency) were identified from the F2 generation based on phenotypic and genotypic characteristics

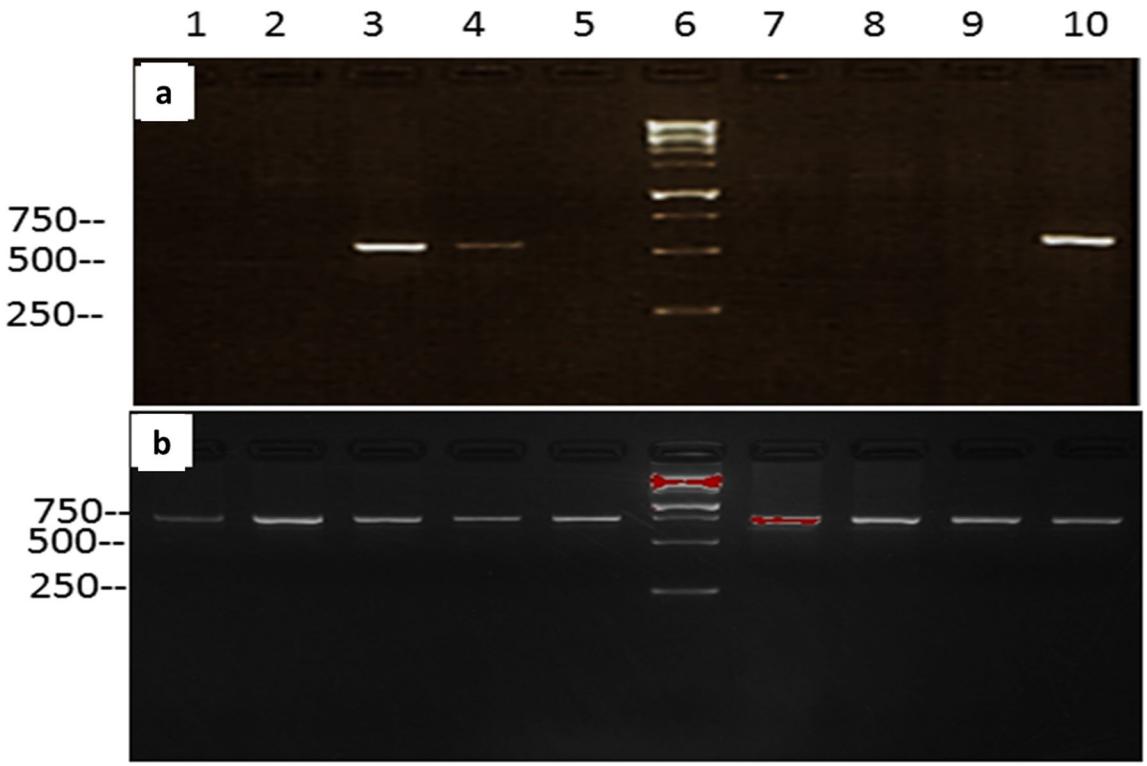

Fig. 2 Genotyping RCS alleles on RCS/mu rats by PCR. **a** A wild-type (WT) allele PCR. **b** A mutant allele PCR. Genotype is determined by the combination of both figures: homozygous = 700 bp product on mutant allele PCR, no amplification on WT allele PCR; heterozygous = 700 bp product on mutant allele PCR and 556 bp product on WT allele PCR. Lanes 1, 2, 5, 7, 8, and 9: homozygous; Lanes 3, 4, and 10: heterozygous.

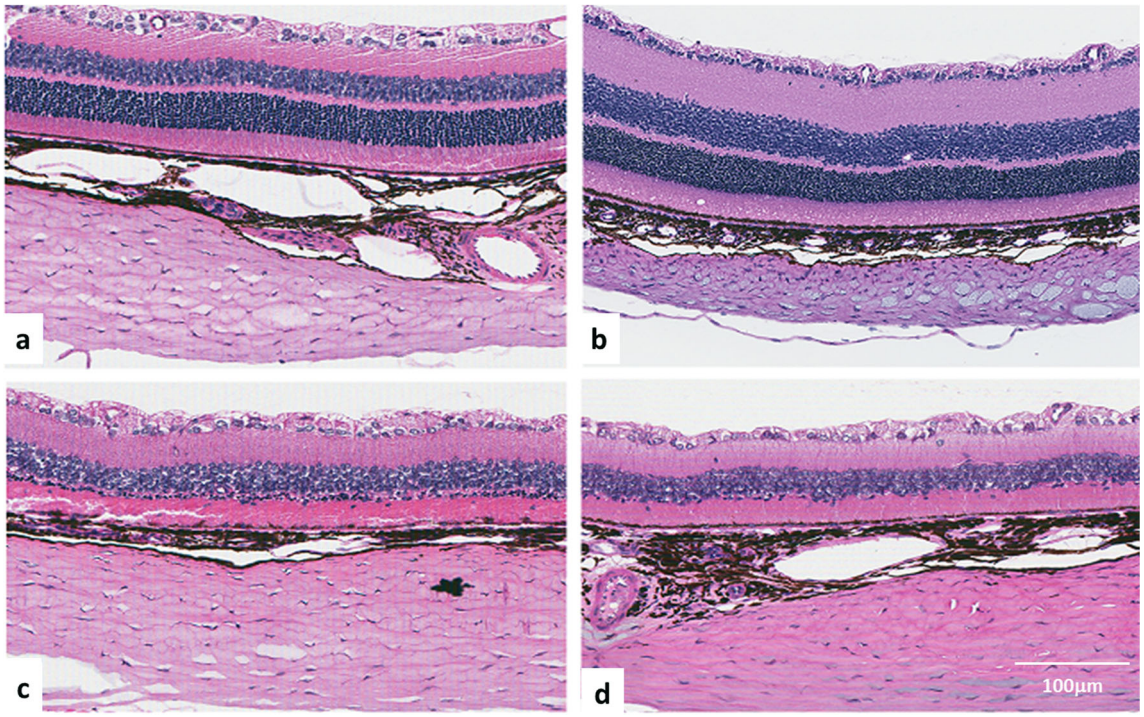

Fig. 3 Photoreceptor degeneration in immunodeficient RCS rats evaluated based on histological examination. Histological assessment of the tissue samples performed at postnatal age of P28 (**b**), 2.5 months (**c**), and 5 months (**d**). Histology of an age-matched (5 months old) non-dystrophic immunodeficient rat (control rat) is also shown in (**a**) for comparison

RCS rats showed considerably low scotopic and photopic A- and B-wave amplitudes. The scotopic A-wave and B-wave and photopic B-wave amplitudes were significantly decreased as the rats aged and reached baseline level by 3 to 4 months of age (Fig. 7). The size of photopic A-wave was too small to demonstrate a clear trend.

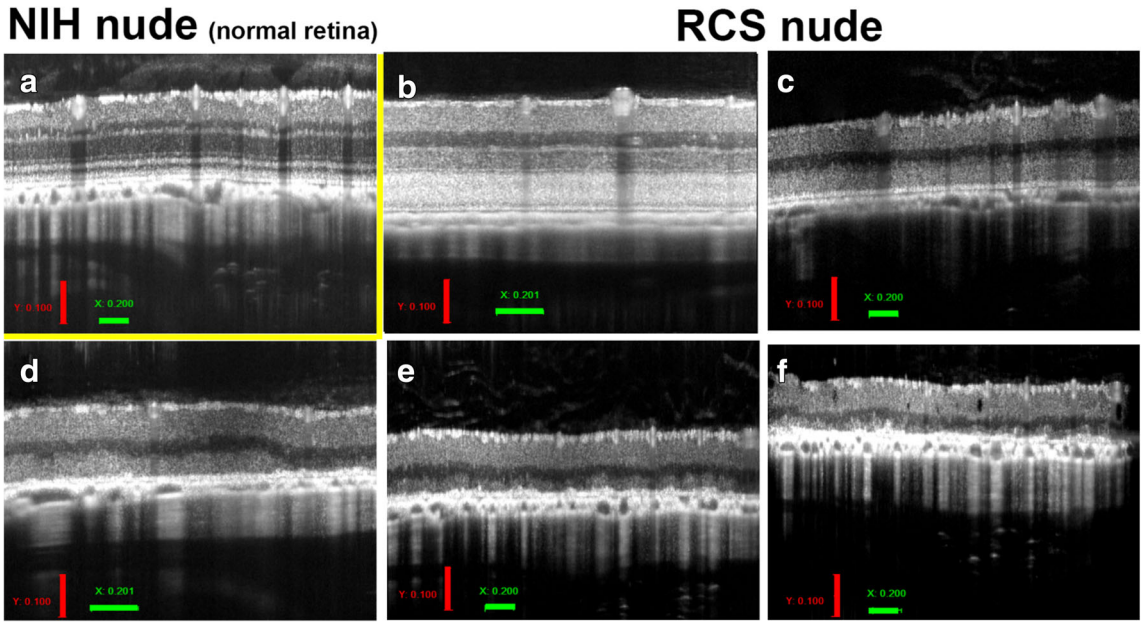

Fig. 4 OCT vertical scan images showing loss of retinal thickness in immunodeficient RCS rats. Image of dystrophic immunodeficient RCS rats at postnatal age of 1 month (**b**) showed retinal thickness comparable to that of non-dystrophic immunodeficient rat (athymic nude rat) (**a**). Loss of retinal thickness was apparent in immunodeficient RCS rats beginning 2 months of age (**c**) that consistently progressed when tested at later time points: 3.5 months (**d**), 5 months (**e**), and 7.5 months (**f**)

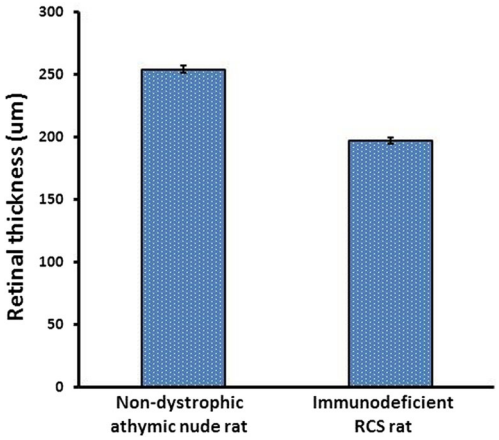

Fig. 5 Retinal thickness measurements using OCT vertical scan images. Significant loss of retinal thickness ($p < 0.001$, Student t test, mean ± SEM, $n = 6$) was observed in immunodeficient RCS rats compared to age-matched non-dystrophic athymic nude rats assessed at the age of 3 months

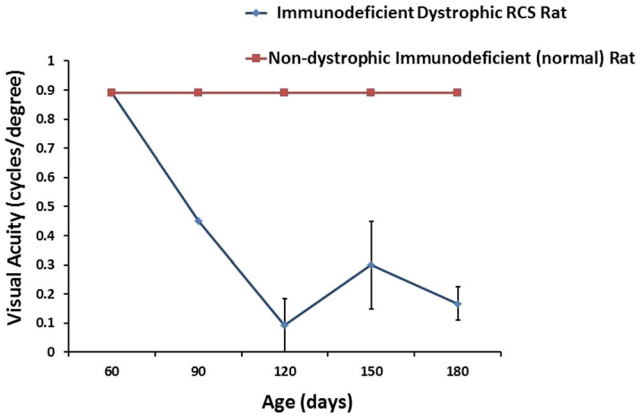

Fig. 6 OKN testing to assess visual functional changes in immunodeficient RCS rats. Visual behavioral assessment based on optokinetic (OKN) testing was performed in dystrophic immunodeficient RCS rats and age-matched non-dystrophic immunodeficient rats at various postnatal (P) time points. After the age of P60, visual acuity decreased considerably in immunodeficient RCS rats, whereas no differences were observed in the control group

Progressive visual loss in immunodeficient RCS rats demonstrated by superior colliculus electrophysiology

Electrophysiological mapping of the SC visual activity demonstrated progressive loss visual function and development of a scotoma in immunodeficient RCS rats which is typical for its non-immunodeficient counterparts [43]. SC visual activity was considerably attenuated at 8 weeks of age. When tested at P180 (24 weeks of age), the presence of a large scotoma was apparent in the SC with most of the SC surface devoid of any light-evoked activity even at high luminescent levels (Fig. 8).

Transplantation studies showed survival of human-derived grafts in immunodeficient RCS rats

Athymic nude rats generally show only mild immune response to xenografts because of their absence of T cells and lack of natural cell-mediated cytotoxicity. To test whether our new rat model (immunodeficient RCS rats) maintains low immune cell-mediated reactions, iPS-RPE and hESC-RPE cells were injected into the subretinal space of double homozygous and founder RCS rats. Histological evaluation of the implanted eyes showed that human-derived iPS-RPE cells well survived in the subretinal space of immunodeficient RCS at 6-month post-injection and were expected to survive longer (Figs. 9 and 10). At 1 month time point, the injected hESC-RPE cells showed good survival in the eyes of both immunodeficient and non-immunodeficient strains. In these rats, considerably less expression of CD68, a macrophage marker, and GFAP, a retinal glial marker, was observed (Fig. 10). The above data suggests lower immune reaction to xenografts in immunodeficient RCS rats. At 6 month post-surgery, no major difference in macrophage (CD68) and retinal glial cells (GFAP) was observed either in the RPE injection area (Fig. 9) or non-injection sites (data not shown), compared to non-injected immunodeficient RCS rats. The expression of immunological markers comparable to the control group suggests absence of apparent chronic inflammation induced by xenografts.

Discussion

In the present study, a new immunodeficient RCS rat model was created. Manifestation of RCS characteristics in this new rat model is demonstrated based on PCR analysis, visual functional assessments, and histological evaluation. This study also demonstrated success of xenograft experiments in this new rat model without administering immunosuppressant drugs. Immunodeficient RD models are valuable for xenograft experiments since most of the preclinical investigational new drug (IND) studies based on cell replacement therapies require experiments conducted using both immunodeficient models and disease models. In the absence of such double homozygous models, non-immunodeficient animals are subjected to severe immunosuppression regimes to avoid graft rejection. For example, our preclinical studies of hESC-RPE implantation-utilized dystrophic RCS rats subjected to systemic administration of dexamethasone and cyclosporine [45]. Other investigators also employed a similar approach in several previous studies [46–54].

The athymic nude rat (Foxn1rnu/rnu) is a popular model to test xenografts derived from human tissue [47, 55–58]. However, since it has a normal retina, it is difficult to evaluate the visual functional benefits of the transplants. The RCS rat which is an RPE dysfunction model has been widely used for assessing cell-based therapies, especially in RPE replacement studies [15, 19, 59]. In these studies, the animals were immunosuppressed using drugs to minimize the tissue rejection and

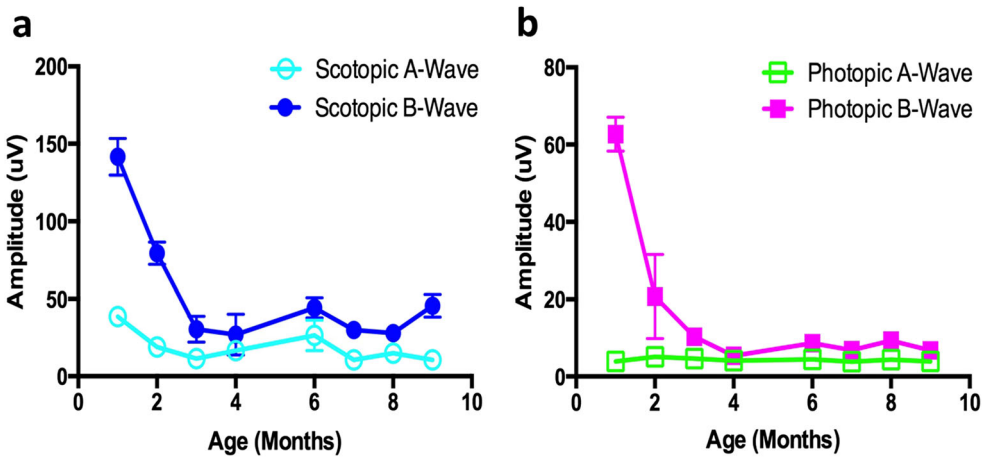

Fig. 7 ERG assessments in immunodeficient RCS rats. Electroretinography recording in RCS nude rats at various postnatal time points. Scotopic A- and B-waves (**a**) and photopic A- and B-waves (**b**) were conducted with flash stimuli intensities at 25 cd/m^2. Progressive decrease of A-wave and B-wave responses was observed in immunodeficient RCS rats. Mean ± SEM, $n = 13$

to enable faithful assessment of the transplant effects [15, 32, 60, 61]. Based on the studies conducted in our laboratory, administration of immunosuppressants is labor intensive and may cause additional pain and discomfort to the animals. Administration of immunosuppressant may negatively influence the health of the recipient, especially with long-term use [62, 63]. In a recent investigation, standard regimen of cyclosporine A plus dexamethasone was administered to RCS rats that caused systemic side effects and depressed scores on behavioral and electrophysiological testing [33].

In the present investigation, we were able to confirm the dystrophic features of the new rat model based on genotyping of the MerTK gene. Expression of disease condition was confirmed by histological and visual functional tests. To produce

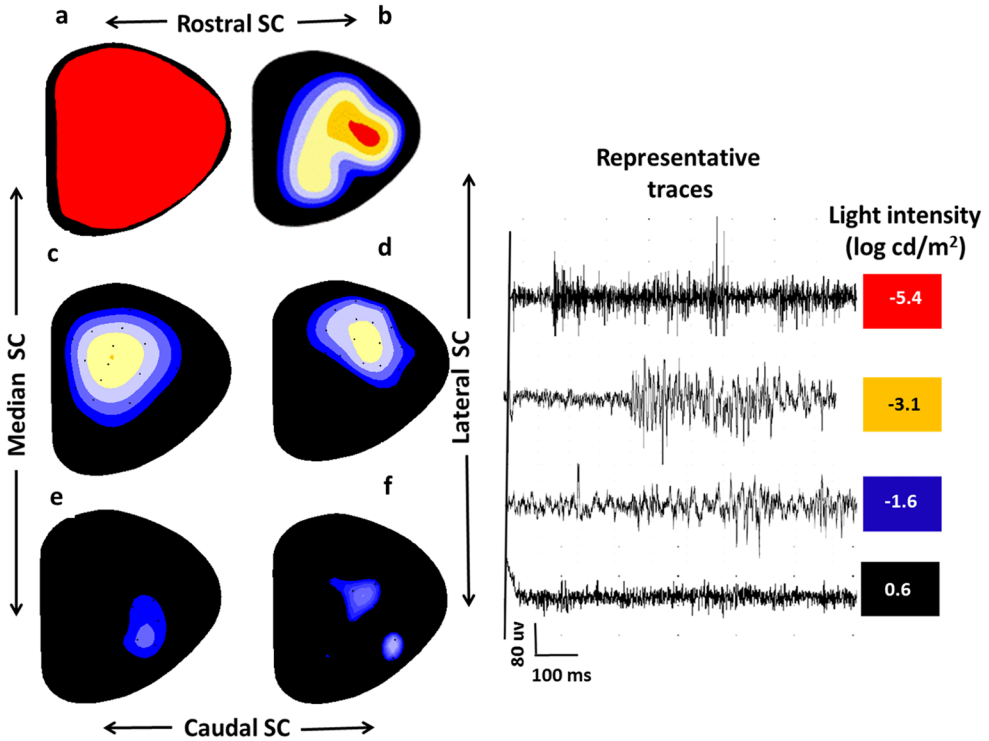

Fig. 8 Superior colliculus (SC) electrophysiology to assess visual functional changes in higher visual areas. Diagrammatic representation of luminance threshold map of the SC in immunodeficient dystrophic RCS rats. The responses were recorded at different light level stimulation (0.6 to 5.4 log cd/m^2) from the age of postnatal (P) 2 to 6 month. **a** Normal (non-dystrophic) athymic nude rat at P90. **b** Immunodeficient dystrophic RCS rat P60. **c** Immunodeficient dystrophic RCS rat P90. **d** Immunodeficient dystrophic RCS rat P120. **e** Immunodeficient dystrophic RCS rat P150. **f** Immunodeficient dystrophic RCS rat P180. Different colors represent areas responding at different light intensity stimuli. Black area means light responses absent. Representative traces are from a 2-month-old immunodeficient dystrophic RCS rat

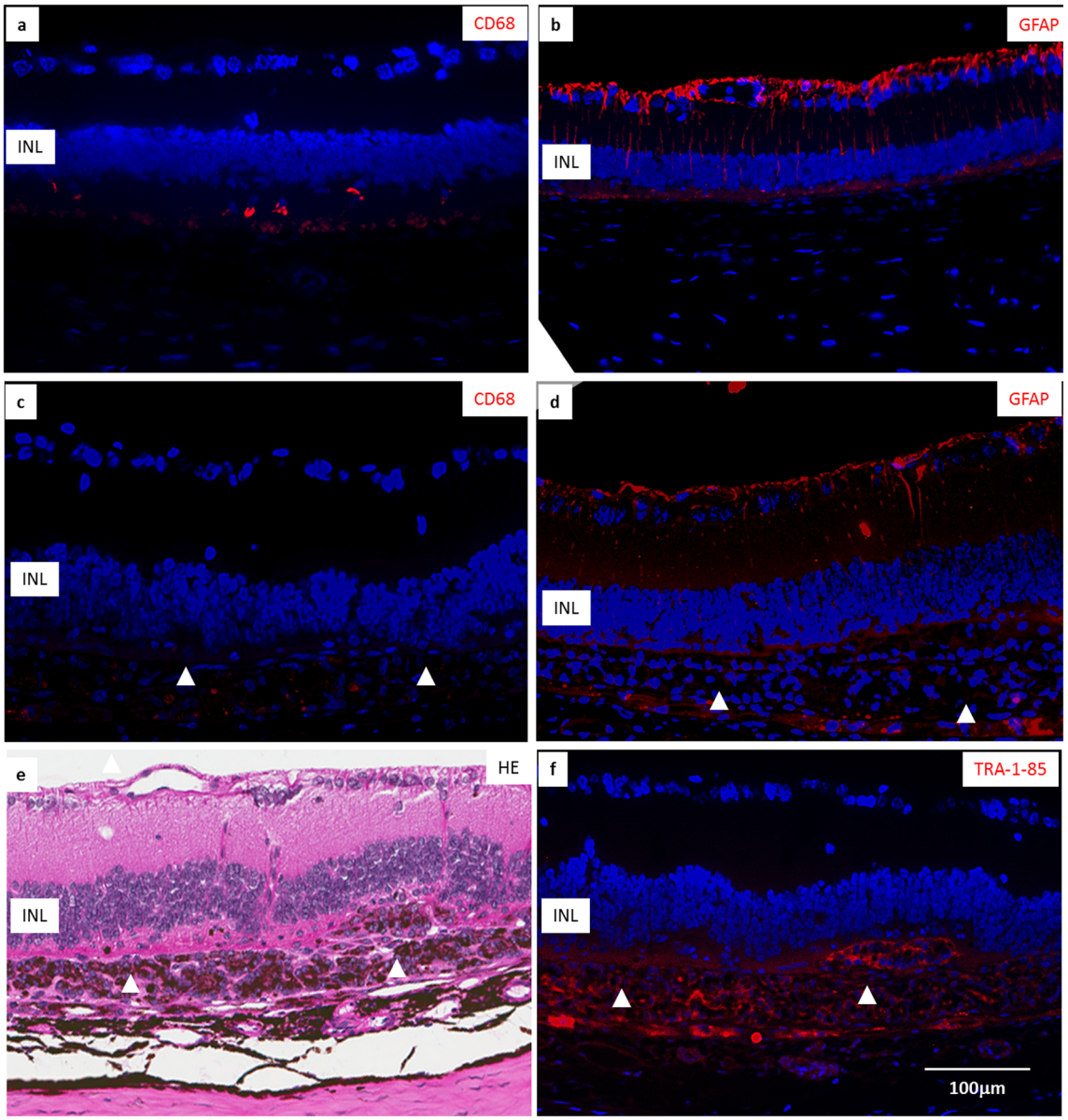

Fig. 9 Xenograft studies in immunodeficient RCS rats using iPS-RPE suspension injection. H&E and immunofluorescent-stained images demonstrate the long-term survival of implanted human cells and no increased immune reaction against implanted cells. The images show no difference in the expression of CD68 (macrophages) and GFAP (glial cells) in xenograft retinas compared to the non-implanted control retinas. Presence of the human-derived RPE cells (TRA-185) was observed in the subretinal space at 6 months post-surgery. **a** CD68, control; **b** GFAP, control; **c** CD68, cell implanted; **d** GFAP, cell implanted; **e** H&E, cell implanted; **f** TRA-1-85 (human marker), cell implanted. White triangles: implanted human RPE cells

immunodeficient RCS pups, double homozygous males were used for breeding, but the females used were heterozygous for immunodeficiency and homozygous for the RCS mutation. Females heterozygous for immunodeficiency was chosen since their homozygous counterparts are known to be incapable of raising pups. As expected, approximately 50% of the progeny were double homozygous (immunodeficient RCS), whereas the other 50% of the pups were non-immunodeficient (heterozygous for immunodeficiency) but homozygous for RCS mutation. Since the immunodeficient status of the animals was easily discernible based on phenotypic expression (hair loss), no separate genotypic tests were conducted for assessing their immunodeficiency status.

The dystrophic status of the double homozygous (immunodeficient and dystrophic) rats was established based on multiple test modalities. Histological assessments showed that the progression of the RD condition in this new model is comparable to their non-immunodeficient counterparts. The above disease features further confirmed by OCT imaging are in agreement with previous investigations conducted in non-immunodeficient dystrophic RCS rats [26–30].

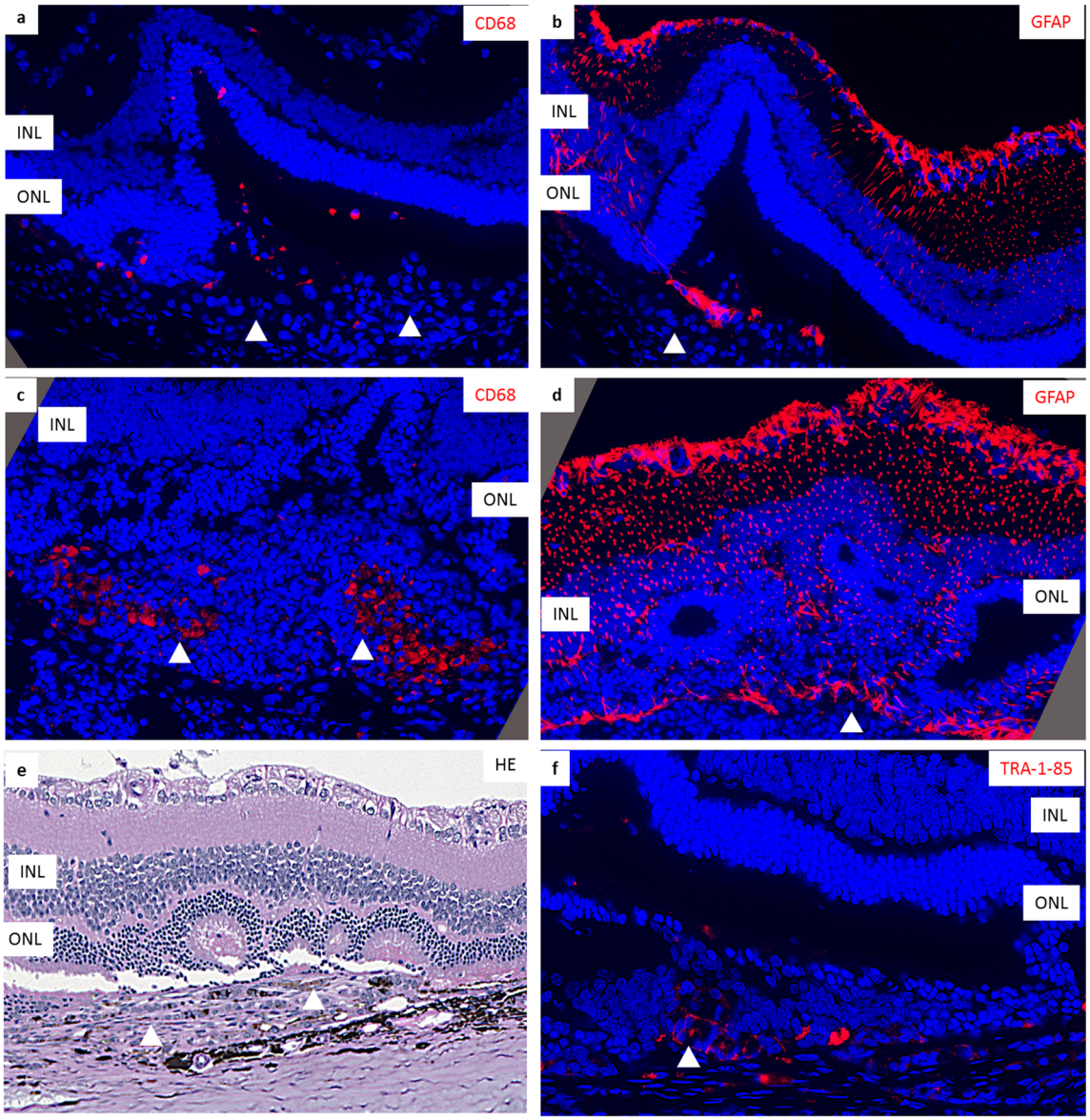

Fig. 10 Comparison of immunological reactions in immunodeficient RCS rats and founder RCS rats following hESC-RPE cell suspension injection. H&E staining and TRA-185 staining demonstrated presence of hESC-RPE cells in both immunodeficient RCS retinas and non-immunodeficient RCS retinas at 1 month after hESC-RPE cell suspension injection. Lesser expression of CD68 (macrophages) and GFAP (glial cells) was observed in immunodeficient RCS retinas compared to the non-immunodeficient strain. **a**, **b** Immunodeficent RCS rats. **c**, **d** Non-immunodeficient founder strain. **e** H&E cell implanted, **f** TRA-1-85 (human marker) cell implanted. White triangles: implanted hESC-RPE cells

For visual functional assessment, we used behavioral and electrophysiological means. The OKN visual assessment demonstrated visual functional loss in the double homozygous individuals as observed in non-immunodeficient dystrophic RCS rats [45]. Consistent with the histology data, ERG testing (scotopic and photopic) also demonstrated progressive attenuation of retinal visual activity that became almost undetectable by the age of 4 months. The above pattern of visual function loss is comparable to the previous observations in non-immunodeficient RCS rats [64–66]. Electrophysiological mapping of the SC also revealed loss of visual function as reported in earlier investigations using non-immunodeficient RCS rats [43, 44, 67].

Most of the investigations involving stem cell-derived therapeutics require testing of the final product in immunodeficient animals to rule out the possibility of tumorigenicity. In our previous investigation, hESC-RPE implants were tested for tumorigenicity using athymic nude rats. This study established absence of tumor formation and immune rejection by hESC-RPE implants [16]. Our new animal model was also tested for immunological reactions by transplanting human-derived cells (iPS-RPE and hESC-RPE). Our studies demonstrated high survival of xenografts in this new RD model in the absence of external immunosuppressant agents. The surviving cells expressed RPE markers and human markers as reported in our previous

investigations where systemic administration of immunosuppressant was employed [45]. Further, less immunological reaction (based on CD 68 and GFAP expression) was observed in immunodeficient strains compared to their non-immunodeficient counterparts. It is possible that survival of the transplant may not always be indicative of visual functional improvements as evidenced by CNT treatment studies where photoreceptor preservation was observed but visual function was not improved accordingly [68]. The focus of our next study will be to assess how the functionality of the transplanted human-derived RPE cells is affected in this new animal model.

In conclusion, our new rat model showing dystrophic features of RCS rats and immunodeficiency status of athymic nude rats is useful for studying the survival and functionality of human-derived cells. Importantly, this new model provides a desirable RD rat model to conduct cell transplantation experiments without involving the adverse effects of immunosuppression. By using this model, it is possible to reduce the total animal number and number of study groups leading to faster completion of research projects. Based on this, IND-enabling preclinical studies can be much faster and cost-effective, and ethical concerns related to the use of laboratory animals can be considerably reduced.

Acknowledgements This study was supported by CIRM TR4-06648 (MJS), CIRM DT3 (MSH), Bright Focus Foundation (BBT), and Research to Prevent Blindness (USC Roski Eye Institute). We want to thank Dr. Kapil Bharti (National Institute of Health, Bethesda, MD, USA) for providing the iPS-RPE, Xiaopeng Wang (USC), and Bryce McLelland, Anuradha Mathur, Jessica Quynh Huong Duong, Marissa Mahtob Marie Monazzami, and Luxi Zhang (UC Irvine) for technical assistance.

Funding Supported by CIRM (MJS, MSH, DRH), Bright Focus Foundation (BBT), and Research to Prevent Blindness (USC Roski Eye Institute). The sponsor had no role in the design or conduct of this research.

Compliance with ethical standards

Conflict of interest MJS has proprietary interest in the instrument and method for transplanting retinal sheets (Ocular Transplantation LLC). MSH and DRH are co-founders and consultants to Regenerative Patch Technologies (RPT). The other authors certify that they have no affiliations with or involvement in any organization or entity with any financial interest (such as honoraria; educational grants; participation in speakers' bureaus; membership, employment, consultancies, stock ownership, or other equity interest; and expert testimony or patent-licensing arrangements) or non-financial interest (such as personal or professional relationships, affiliations, knowledge, or beliefs) in the subject matter or materials discussed in this manuscript.

Ethical approval All applicable international, national, and/or institutional guidelines for the care and use of the animals were followed. All procedures performed in studies involving animals were in accordance with the ethical standards of University of Southern California Institutional Animal Care and Use Committee (IACUC).

References

1. Garg A, Yang J, Lee W, Tsang SH (2017) Stem cell therapies in retinal disorders. Cells 6. DOI https://doi.org/10.3390/cells6010004
2. Jayakody SA, Gonzalez-Cordero A, Ali RR, Pearson RA (2015) Cellular strategies for retinal repair by photoreceptor replacement. Prog Retin Eye Res 46:31–66. https://doi.org/10.1016/j.preteyeres.2015.01.003
3. Jones MK, Lu B, Girman S, Wang S (2017) Cell-based therapeutic strategies for replacement and preservation in retinal degenerative diseases. Prog Retin Eye Res 58:1–27. https://doi.org/10.1016/j.preteyeres.2017.01.004
4. Seiler MJ, Aramant RB (2012) Cell replacement and visual restoration by retinal sheet transplants. Prog Retin Eye Res 31:661–687. https://doi.org/10.1016/j.preteyeres.2012.06.003
5. Quigley HA, Iglesia DS (2004) Stem cells to replace the optic nerve. Eye (Lond) 18:1085–1088. https://doi.org/10.1038/sj.eye.6701577
6. Thomas BB, Aramant RB, Sadda SR, Seiler MJ (2006) Retinal transplantation. A treatment strategy for retinal degenerative diseases. Adv Exp Med Biol 572:367–376
7. Thomas BB, Seiler MJ, Sadda SR, Aramant RB (2004) Superior colliculus responses to light - preserved by transplantation in a slow degeneration rat model. Exp Eye Res 79:29–39. https://doi.org/10.1016/j.exer.2004.02.016
8. Seiler MJ, Lin RE, McLelland BT, Mathur A, Lin B, Sigman J, De Guzman AT, Kitzes LM, Aramant RB, Thomas BB (2017) Vision recovery and connectivity by fetal retinal sheet transplantation in an immunodeficient retinal degenerate rat model. Invest Ophthalmol Vis Sci 58:614–630. https://doi.org/10.1167/iovs.15-19028
9. Radtke ND, Aramant RB, Petry HM, Green PT, Pidwell DJ, Seiler MJ (2008) Vision improvement in retinal degeneration patients by implantation of retina together with retinal pigment epithelium. Am J Ophthalmol 146:172–182. https://doi.org/10.1016/j.ajo.2008.04.009
10. D'Cruz PM, Yasumura D, Weir J, Matthes MT, Abderrahim H, LaVail MM, Vollrath D (2000) Mutation of the receptor tyrosine kinase gene Mertk in the retinal dystrophic RCS rat. Hum Mol Genet 9:645–651
11. Vollrath D, Feng W, Duncan JL, Yasumura D, D'Cruz PM, Chappelow A, Matthes MT, Kay MA, LaVail MM (2001) Correction of the retinal dystrophy phenotype of the RCS rat by viral gene transfer of Mertk. Proc Natl Acad Sci U S A 98:12584–12589. https://doi.org/10.1073/pnas.221364198
12. Liu C, Li Y, Peng M, Laties AM, Wen R (1999) Activation of caspase-3 in the retina of transgenic rats with the rhodopsin mutation s334ter during photoreceptor degeneration. J Neurosci 19:4778–4785
13. Ray A, Sun GJ, Chan L, Grzywacz NM, Weiland J, Lee EJ (2010) Morphological alterations in retinal neurons in the S334ter-line3 transgenic rat. Cell Tissue Res 339:481–491. https://doi.org/10.1007/s00441-009-0916-5
14. Zhu CL, Ji Y, Lee EJ, Grzywacz NM (2013) Spatiotemporal pattern of rod degeneration in the S334ter-line-3 rat model of retinitis pigmentosa. Cell Tissue Res 351:29–40. https://doi.org/10.1007/s00441-012-1522-5
15. Carr AJ, Vugler AA, Hikita ST, Lawrence JM, Gias C, Chen LL, Buchholz DE, Ahmado A, Semo M, Smart MJ, Hasan S, da Cruz L, Johnson LV, Clegg DO, Coffey PJ (2009) Protective effects of human iPS-derived retinal pigment epithelium cell transplantation in the retinal dystrophic rat. PLoS One 4:e8152. https://doi.org/10.1371/journal.pone.0008152
16. Diniz B, Thomas P, Thomas B, Ribeiro R, Hu Y, Brant R, Ahuja A, Zhu D, Liu L, Koss M, Maia M, Chader G, Hinton DR, Humayun MS (2013) Subretinal implantation of retinal pigment epithelial

cells derived from human embryonic stem cells: improved survival when implanted as a monolayer. Invest Ophthalmol Vis Sci 54: 5087–5096. https://doi.org/10.1167/iovs.12-11239
17. Gregory-Evans K, Chang F, Hodges MD, Gregory-Evans CY (2009) Ex vivo gene therapy using intravitreal injection of GDNF-secreting mouse embryonic stem cells in a rat model of retinal degeneration. Mol Vis 15:962–973
18. Park UC, Cho MS, Park JH, Kim SJ, Ku SY, Choi YM, Moon SY, Yu HG (2011) Subretinal transplantation of putative retinal pigment epithelial cells derived from human embryonic stem cells in rat retinal degeneration model. Clin Exp Reprod Med 38:216–221. https://doi.org/10.5653/cerm.2011.38.4.216
19. Pinilla I, Cuenca N, Sauve Y, Wang S, Lund RD (2007) Preservation of outer retina and its synaptic connectivity following subretinal injections of human RPE cells in the Royal College of Surgeons rat. Exp Eye Res 85:381–392. https://doi.org/10.1016/j.exer.2007.06.002
20. Wang S, Girman S, Lu B, Bischoff N, Holmes T, Shearer R, Wright LS, Svendsen CN, Gamm DM, Lund RD (2008) Long-term vision rescue by human neural progenitors in a rat model of photoreceptor degeneration. Invest Ophthalmol Vis Sci 49:3201–3206. https://doi.org/10.1167/iovs.08-1831
21. Yanai A, Hafeli UO, Metcalfe AL, Soema P, Addo L, Gregory-Evans CY, Po K, Shan X, Moritz OL, Gregory-Evans K (2012) Focused magnetic stem cell targeting to the retina using superparamagnetic iron oxide nanoparticles. Cell Transplant 21: 1137–1148. https://doi.org/10.3727/096368911x627435
22. Lin TC, Seiler MJ (2017) Assessment of safety and functional efficacy of stem cell-based therapeutic approaches using retinal degenerative animal models. Stem Cells Int 2017:9428176. https://doi.org/10.1155/2017/9428176
23. Nandrot EF, Dufour EM (2010) Mertk in daily retinal phagocytosis: a history in the making. Adv Exp Med Biol 664:133–140. https://doi.org/10.1007/978-1-4419-1399-9_16
24. Ambati J, Fowler BJ (2012) Mechanisms of age-related macular degeneration. Neuron 75:26–39. https://doi.org/10.1016/j.neuron.2012.06.018
25. McGill TJ, Cottam B, Lu B, Wang S, Girman S, Tian C, Huhn SL, Lund RD, Capela A (2012) Transplantation of human central nervous system stem cells - neuroprotection in retinal degeneration. Eur J Neurosci 35:468–477. https://doi.org/10.1111/j.1460-9568.2011.07970.x
26. DiLoreto DA Jr, del Cerro C, Cox C, del Cerro M (1998) Changes in visually guided behavior of Royal College of Surgeons rats as a function of age: a histologic, morphometric, and functional study. Invest Ophthalmol Vis Sci 39:1058–1063
27. Feng W, Yasumura D, Matthes MT, LaVail MM, Vollrath D (2002) Mertk triggers uptake of photoreceptor outer segments during phagocytosis by cultured retinal pigment epithelial cells. J Biol Chem 277:17016–17022. https://doi.org/10.1074/jbc.M107876200
28. Mullen RJ, LaVail MM (1976) Inherited retinal dystrophy: primary defect in pigment epithelium determined with experimental rat chimeras. Science 192:799–801
29. Goldman AI, O'Brien PJ (1978) Phagocytosis in the retinal pigment epithelium of the RCS rat. Science 201:1023–1025
30. Sauve Y, Girman SV, Wang S, Lawrence JM, Lund RD (2001) Progressive visual sensitivity loss in the Royal College of Surgeons rat: perimetric study in the superior colliculus. Neuroscience 103:51–63
31. Kamao H, Mandai M, Okamoto S, Sakai N, Suga A, Sugita S, Kiryu J, Takahashi M (2014) Characterization of human induced pluripotent stem cell-derived retinal pigment epithelium cell sheets aiming for clinical application. Stem Cell Rep 2:205–218. https://doi.org/10.1016/j.stemcr.2013.12.007
32. Lu B, Malcuit C, Wang S, Girman S, Francis P, Lemieux L, Lanza R, Lund R (2009) Long-term safety and function of RPE from human embryonic stem cells in preclinical models of macular degeneration. Stem Cells 27:2126–2135. https://doi.org/10.1002/stem.149
33. Cooper AE, Cho JH, Menges S, Masood S, Xie J, Yang J, Klassen H (2016) Immunosuppressive treatment can alter visual performance in the Royal College of Surgeons rat. J Ocul Pharmacol Ther 32:296–303. https://doi.org/10.1089/jop.2015.0134
34. Anderson AJ, Haus DL, Hooshmand MJ, Perez H, Sontag CJ, Cummings BJ (2011) Achieving stable human stem cell engraftment and survival in the CNS: is the future of regenerative medicine immunodeficient? Regen Med 6:367–406. https://doi.org/10.2217/rme.11.22
35. Zhu J, Cifuentes H, Reynolds J, Lamba DA (2017) Immunosuppression via loss of IL2rgamma enhances long-term functional integration of hESC-derived photoreceptors in the mouse retina. Cell Stem Cell 20:374–384 e375. https://doi.org/10.1016/j.stem.2016.11.019
36. Seiler MJ, Aramant RB, Jones MK, Ferguson DL, Bryda EC, Keirstead HS (2014) A new immunodeficient pigmented retinal degenerate rat strain to study transplantation of human cells without immunosuppression. Graefes Arch Clin Exp Ophthalmol 252: 1079–1092. https://doi.org/10.1007/s00417-014-2638-y
37. Hirasawa T, Ohara T, Makino S (1997) Genetic typing of the mouse ob mutation by PCR and restriction enzyme analysis. Exp Anim 46: 75–78
38. Thomas BB, Seiler MJ, Sadda SR, Coffey PJ, Aramant RB (2004) Optokinetic test to evaluate visual acuity of each eye independently. J Neurosci Methods 138:7–13. https://doi.org/10.1016/j.jneumeth.2004.03.007
39. Siminoff R, Schwassmann HO, Kruger L (1966) An electrophysiological study of the visual projection to the superior colliculus of the rat. J Comp Neurol 127:435–444. https://doi.org/10.1002/cne.901270402
40. Thomas BB, Aramant RB, Sadda SR, Seiler MJ (2005) Light response differences in the superior colliculus of albino and pigmented rats. Neurosci Lett 385:143–147. https://doi.org/10.1016/j.neulet.2005.05.034
41. Ferrer M, Corneo B, Davis J, Wan Q, Miyagishima KJ, King R, Maminishkis A, Marugan J, Sharma R, Shure M, Temple S, Miller S, Bharti K (2014) A multiplex high-throughput gene expression assay to simultaneously detect disease and functional markers in induced pluripotent stem cell-derived retinal pigment epithelium. Stem Cells Transl Med 3:911–922. https://doi.org/10.5966/sctm.2013-0192
42. Miyagishima KJ, Wan Q, Corneo B, Sharma R, Lotfi MR, Boles NC, Hua F, Maminishkis A, Zhang C, Blenkinsop T, Khristov V, Jha BS, Memon OS, D'Souza S, Temple S, Miller SS, Bharti K (2016) In pursuit of authenticity: induced pluripotent stem cell-derived retinal pigment epithelium for clinical applications. Stem Cells Transl Med. https://doi.org/10.5966/sctm.2016-0037
43. Woch G, Aramant RB, Seiler MJ, Sagdullaev BT, McCall MA (2001) Retinal transplants restore visually evoked responses in rats with photoreceptor degeneration. Invest Ophthalmol Vis Sci 42: 1669–1676
44. Sagdullaev BT, Aramant RB, Seiler MJ, Woch G, McCall MA (2003) Retinal transplantation-induced recovery of retinotectal visual function in a rodent model of retinitis pigmentosa. Invest Ophthalmol Vis Sci 44:1686–1695
45. Thomas BB, Zhu D, Zhang L, Thomas PB, Hu Y, Nazari H, Stefanini F, Falabella P, Clegg DO, Hinton DR, Humayun MS (2016) Survival and functionality of hESC-derived retinal pigment epithelium cells cultured as a monolayer on polymer substrates transplanted in RCS rats. Invest Ophthalmol Vis Sci 57:2877–2887. https://doi.org/10.1167/iovs.16-19238
46. Clarke L, Ballios BG, van der Kooy D (2012) Generation and clonal isolation of retinal stem cells from human embryonic stem

cells. Eur J Neurosci 36:1951–1959. https://doi.org/10.1111/j.1460-9568.2012.08123.x
47. Guest JD, Rao A, Olson L, Bunge MB, Bunge RP (1997) The ability of human Schwann cell grafts to promote regeneration in the transected nude rat spinal cord. Exp Neurol 148:502–522. https://doi.org/10.1006/exnr.1997.6693
48. Hambright D, Park KY, Brooks M, McKay R, Swaroop A, Nasonkin IO (2012) Long-term survival and differentiation of retinal neurons derived from human embryonic stem cell lines in unimmunosuppressed mouse retina. Mol Vis 18:920–936
49. Lamba DA, Karl MO, Ware CB, Reh TA (2006) Efficient generation of retinal progenitor cells from human embryonic stem cells. Proc Natl Acad Sci U S A 103:12769–12774. https://doi.org/10.1073/pnas.0601990103
50. Lamba DA, McUsic A, Hirata RK, Wang PR, Russell D, Reh TA (2010) Generation, purification and transplantation of photoreceptors derived from human induced pluripotent stem cells. PLoS One 5:e8763. https://doi.org/10.1371/journal.pone.0008763
51. Meyer JS, Howden SE, Wallace KA, Verhoeven AD, Wright LS, Capowski EE, Pinilla I, Martin JM, Tian S, Stewart R, Pattnaik B, Thomson JA, Gamm DM (2011) Optic vesicle-like structures derived from human pluripotent stem cells facilitate a customized approach to retinal disease treatment. Stem Cells 29:1206–1218. https://doi.org/10.1002/stem.674
52. Tucker BA, Park IH, Qi SD, Klassen HJ, Jiang C, Yao J, Redenti S, Daley GQ, Young MJ (2011) Transplantation of adult mouse iPS cell-derived photoreceptor precursors restores retinal structure and function in degenerative mice. PLoS One 6:e18992. https://doi.org/10.1371/journal.pone.0018992
53. Vugler AA (2010) Progress toward the maintenance and repair of degenerating retinal circuitry. Retina 30:983–1001. https://doi.org/10.1097/IAE.0b013e3181e2a680
54. Yue F, Johkura K, Shirasawa S, Yokoyama T, Inoue Y, Tomotsune D, Sasaki K (2010) Differentiation of primate ES cells into retinal cells induced by ES cell-derived pigmented cells. Biochem Biophys Res Commun 394:877–883. https://doi.org/10.1016/j.bbrc.2010.03.008
55. Nasonkin I, Mahairaki V, Xu L, Hatfield G, Cummings BJ, Eberhart C, Ryugo DK, Maric D, Bar E, Koliatsos VE (2009) Long-term, stable differentiation of human embryonic stem cell-derived neural precursors grafted into the adult mammalian neostriatum. Stem Cells 27:2414–2426. https://doi.org/10.1002/stem.177
56. Aramant RB, Seiler MJ (2002) Transplanted sheets of human retina and retinal pigment epithelium develop normally in nude rats. Exp Eye Res 75:115–125
57. Granholm AC, Eriksdotter-Nilsson M, Stromberg I, Stieg P, Seiger A, Bygdeman M, Geffard M, Oertel W, Dahl D, Olson L et al (1989) Morphological and electrophysiological studies of human hippocampal transplants in the anterior eye chamber of athymic nude rats. Exp Neurol 104:162–171
58. Hall M, Wang Y, Granholm AC, Stevens JO, Young D, Hoffer BJ (1992) Comparison of fetal rabbit brain xenografts to three different strains of athymic nude rats: electrophysiological and immunohistochemical studies of intraocular grafts. Cell Transplant 1:71–82
59. Wang S, Lu B, Girman S, Holmes T, Bischoff N, Lund RD (2008) Morphological and functional rescue in RCS rats after RPE cell line transplantation at a later stage of degeneration. Invest Ophthalmol Vis Sci 49:416–421. https://doi.org/10.1167/iovs.07-0992
60. Grisanti S, Szurman P, Jordan J, Kociok N, Bartz-Schmidt KU, Heimann K (2002) Xenotransplantation of retinal pigment epithelial cells into RCS rats. Jpn J Ophthalmol 46:36–44
61. Lund RD, Wang S, Klimanskaya I, Holmes T, Ramos-Kelsey R, Lu B, Girman S, Bischoff N, Sauve Y, Lanza R (2006) Human embryonic stem cell-derived cells rescue visual function in dystrophic RCS rats. Cloning Stem Cells 8:189–199. https://doi.org/10.1089/clo.2006.8.189
62. Cibulskyte D, Kaalund H, Pedersen M, Horlyck A, Marcussen N, Hansen HE, Madsen M, Mortensen J (2005) Chronic cyclosporine nephrotoxicity: a pig model. Transplant Proc 37:3298–3301. https://doi.org/10.1016/j.transproceed.2005.09.004
63. Thliveris JA, Yatscoff RW, Lukowski MP, Copeland KR (1991) Cyclosporine nephrotoxicity–experimental models. Clin Biochem 24:93–95
64. Adachi K, Takahashi S, Yamauchi K, Mounai N, Tanabu R, Nakazawa M (2016) Optical coherence tomography of retinal degeneration in Royal College of Surgeons rats and its correlation with morphology and electroretinography. PLoS One 11:e0162835. https://doi.org/10.1371/journal.pone.0162835
65. Rosch S, Aretzweiler C, Muller F, Walter P (2017) Evaluation of retinal function and morphology of the pink-eyed Royal College of Surgeons (RCS) rat: a comparative study of in vivo and in vitro methods. Curr Eye Res 42:273–281. https://doi.org/10.1080/02713683.2016.1179333
66. Tzameret A, Sher I, Belkin M, Treves AJ, Meir A, Nagler A, Levkovitch-Verbin H, Barshack I, Rosner M, Rotenstreich Y (2014) Transplantation of human bone marrow mesenchymal stem cells as a thin subretinal layer ameliorates retinal degeneration in a rat model of retinal dystrophy. Exp Eye Res 118:135–144. https://doi.org/10.1016/j.exer.2013.10.023
67. Girman SV, Wang S, Lund RD (2005) Time course of deterioration of rod and cone function in RCS rat and the effects of subretinal cell grafting: a light- and dark-adaptation study. Vis Res 45:343–354. https://doi.org/10.1016/j.visres.2004.08.023
68. Birch DG, Bennett LD, Duncan JL, Weleber RG, Pennesi ME (2016) Long-term follow-up of patients with retinitis pigmentosa receiving intraocular ciliary neurotrophic factor implants. Am J Ophthalmol 170:10–14. https://doi.org/10.1016/j.ajo.2016.07.013